Available online at www.sciencedirect.com

SCIENCE DIRECT®

Polymer 46 (2005) 11635–11639

polymer

www.elsevier.com/locate/polymer

Solvent annealing thin films of poly(isoprene-*b*-lactide)

Kevin A. Cavicchi [a], Keith J. Berthiaume [b], Thomas P. Russell [a,*]

[a] *Department of Polymer Science and Engineering, University of Massachusetts Amherst, Amherst, MA 01003, USA*
[b] *Gateway Regional High school, Huntington, MA 01050, USA*

Received 4 August 2005; received in revised form 21 September 2005; accepted 24 September 2005
Available online 19 October 2005

Abstract

The use of solvent annealing to control the microdomain orientation and long-range ordering in poly(isoprene-*b*-D,L-lactide) thin films was investigated using scanning force microscopy and grazing incidence small angle X-ray scattering (GISAXS). Benzene and chloroform were used as annealing solvents. Both were found to improve the long-range order in the films. Additionally, at high concentrations of chloroform in the film, a perpendicular orientation of cylinders was observed where the solvent was able to mediate interfacial interactions sufficiently to prevent a preferential segregation of one of the blocks to the surface. In situ GISAXS measurements made during solvent swelling and evaporation allowed an examination of the film morphology over a wide range of solvent concentrations providing a efficient route to optimize conditions for morphology control by solvent annealing.

Keywords: Copolymer; Solvent; Annealing

1. Introduction

The ability of block copolymers to self-assemble into morphologies having domains tens of nanometers in size makes them ideal materials for the fabrication of nanostructured thin films [1]. Copolymers forming hexagonally packed cylinders are technologically interesting as templates for etch barriers [2], separation membranes [3], or nanoreactors [4]. Two key parameters to control are the orientation of the cylindrical microdomains, since pattern transfer and etching processes require high aspect ratio templates, and long-range order, which is key for addressing each microdomain. In essence, it is necessary to establish conditions under which the self-assembly of the copolymers is directed and self-orienting and the arrays of microdomains formed have long-range order.

The substrate and air interfaces are typically selective to one of the blocks and causes an orientation of the microdomain morphology parallel to the surface. By balancing interfacial interactions [5,6], an orientation of the microdomain morphology normal to the film surface can be achieved. Recent experiments have used this to generate high aspect ratio cylinders via a solvent evaporation process [7]. By swelling a dried film with a good solvent for both blocks, or by casting a thin film from solution, the highly swollen copolymer is disordered. As the solvent evaporates, the concentration of the solvent at the free surface decreases, and the copolymer orders. The solvent mediates the surface energies of both blocks, making them comparable, which leads to an orientation of the microdomains normal to the surface while the remainder of the film is still disordered. The presence of the solvent imparts a high mobility to the copolymer and, if the segmental interactions are sufficiently strong, defects in the packing of the microdomains are rapidly removed at the surface. As the solvent continues to evaporate, an ordering front propagates through the film and the microdomains of the copolymer are templated by the existing microdomain morphology at the surface. This process is akin to classical zone refinement, typically used to produce large-scale single crystals. Consequently, highly oriented arrays of the microdomains are produced with a high degree of lateral order.

In the work of Knoll et al., block copolymer films were swollen with solvent, but the block copolymer remained in the ordered state [8]. After annealing the film at a constant solvent concentration, the solvent was rapidly evaporated, kinetically trapping the morphology. Variations in the thickness were found across the film and at specific thicknesses a normal orientation of the microdomains was obtained. Here, the solvent mediates the interfacial interactions, reducing the preferential segregation of either block to the interface. However, the interfaces are not perfectly neutral. A normal

---

* Corresponding author. Tel.: +1 413 577 1516; fax: +1 413 577 1510.
E-mail address: russell@mail.pse.umass.edu (T.P. Russell).

0032-3861/$ - see front matter © 2005 Elsevier Ltd. All rights reserved.
doi:10.1016/j.polymer.2005.09.072

orientation of the microdomain morphology is only observed when the film thickness is incommensurate with the total film thickness. When the film thickness is commensurate, the microdomains orient parallel to the surface. These observations are in line with the theoretical arguments of Turner [9], Walton et al. [10], Fasolka et al. [11], Huinink et al. [12], and Horvat et al. [6] and the experimental findings of Lambooy et al. [13] and Kellogg et al. [14].

Studies were performed on controlling the orientation of poly(isoprene-*b*-D,L lactide) (PI-*b*-PLA) where the PLA forms cylinders in a matrix of the PI. Due to the strong non-favorable segmental interactions between the blocks ($\chi \sim 0.3$ at 25 °C), the size of the individual cylindrical microdomains can be reduced to several nanometers, while maintaining the microphase separation. PI can also be chemically crosslinked, stabilizing the matrix, and the PLA can be chemically degraded and removed to produce films with arrays of nanopores of uniform size with long-range order. The viability of the solvent-based techniques described above to obtain films with a normal orientation of the cylindrical microdomains was examined for this block copolymer. A key element in these studies was the use of in situ grazing-incidence small-angle X-ray scattering (GISAXS) during swelling and evaporation to examine the film structure.

2. Results and discussion

Fig. 1 shows the scanning force microscope (SFM) phase images of PI-*b*-PLA 6-3 thin films ($t_0 = 100$ nm) prior to and after annealing in a benzene vapor for different lengths of time. In the phase image the more rigid PLA phase appears brighter. The annealing process increases the chain mobility allowing the grains to coarsen such that, with longer annealing times, the grain sizes have increased markedly. However, only a parallel orientation of the cylindrical microdomains is observed.

To monitor film morphology during annealing GISAXS measurements were performed on films during solvent swelling and evaporation. Fig. 2 shows a schematic diagram of the GISAXS experiment. Fig. 3 shows the GISAXS pattern of a film ($t_0 = 100$ nm) upon swelling and evaporation. The patterns are consistent with a parallel orientation of the cylindrical microdomains, as seen in Fig. 3(c). During the entire annealing process only a parallel orientation of the cylindrical microdomains was observed. Reflections can be observed in Fig. 3(b), arising from the hexagonal packing of the parallel cylinders. The intense reflections at $q_z = 0.035$ Å^{-1} arise from the scattering of the incident beam, while the weaker reflections at $q_z = 0.06$ Å^{-1} arise from the scattering of the beam reflected at the silicon surface [15]. Further swelling

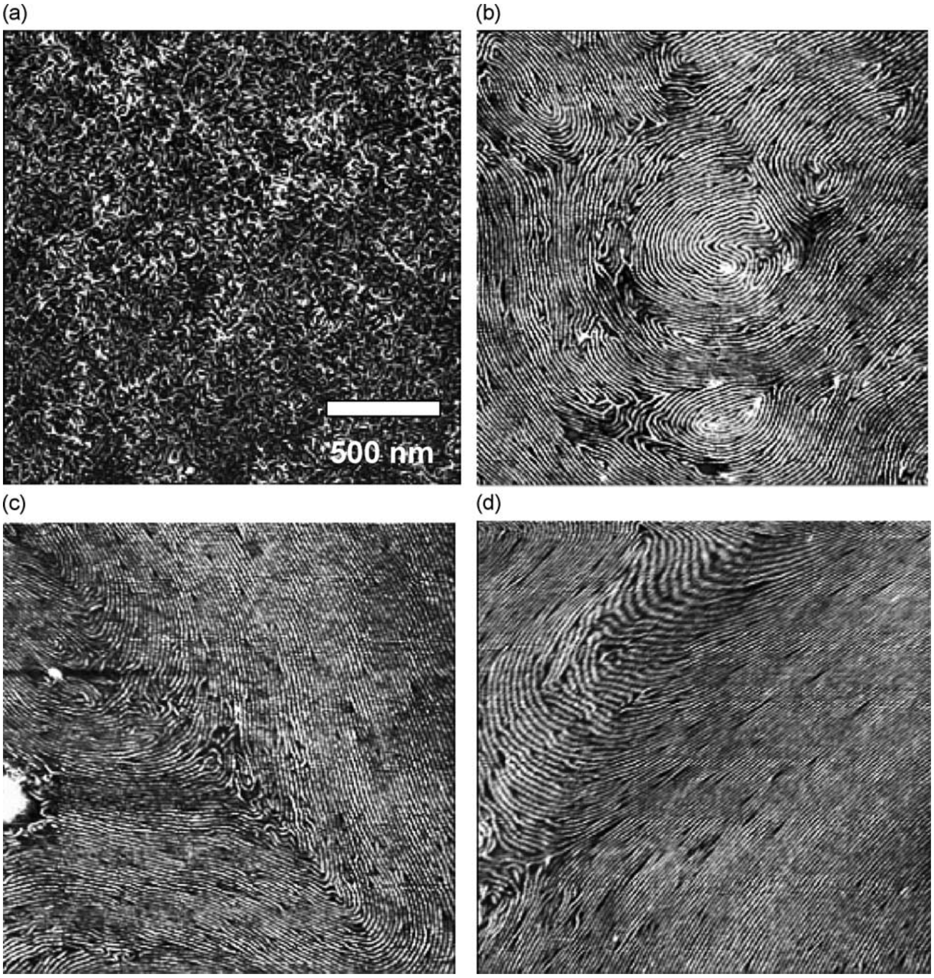

Fig. 1. SFM phase images of 100 nm thick PI-*b*-PLA thin films (a) as-spun and swollen with benzene for (b) 1 min (c) 10 min and (d) 30 min.

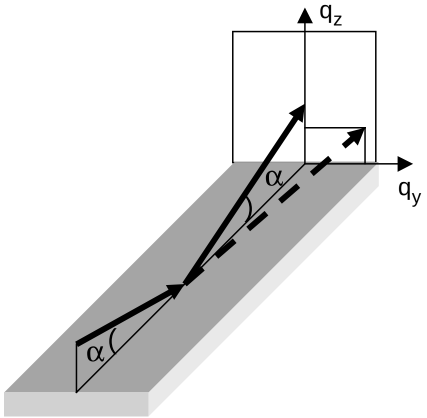

Fig. 2. Schematic representation of the GISAXS experiment. The beam is incident on the sample at an angle α. There is a specular reflection at an angle α. The dotted line indicates an off-specular reflection in the q_y–q_z plane.

disorders the copolymer. Upon solvent evaporation, the block copolymer microphase separates and a parallel orientation of the cylindrical microdomains was again observed. Thus, it is apparent that the solvent does not mediate the surface energies sufficiently as the block copolymer microphase separates, to force an orientation of the microdomains normal to the surface. Yet, it is very apparent that the solvent has induced sufficient mobility to obtain a significant long-range ordering of the copolymer in the plane of the film. To achieve this by thermal means, the temperature of the film would have to be raised above the T_gs of both blocks ($T_{g,PI} = -68$ °C, $T_{g,PLA} = 60$ °C) [16]. With thermally sensitive blocks, as is the case with PI, the solvent-based process shown here, performed at room temperature, has distinct advantages.

Studies were also performed on microphase separated PI-*b*-PLA films that were swollen with chloroform, a good solvent for both blocks. In such films, the mobility of the copolymer is enhanced, interfacial interactions are mediated and, consequently, the commensurability between the total film thickness and the period of the copolymer should dictate the orientation of the microdomains. When commensurate, the microdomains should orient parallel to the film surface and, when incommensurate, the microdomais should orient normal to the film surface. Higher molecular weight PI-*b*-PLA was used in these studies to increase the thickness range over which the microdomains should orient normal to the film surface. For the block copolymers used here, d_{10} was measured to be 16 and 23 nm by SFM for PI-*b*-PLA 6-3 and PI-*b*-PLA 16-6, respectively. While chloroform is a good solvent for both blocks, there are differences in the selectivity of the solvents. The solubility parameters of PI and PLA are 16.9 and 19.7 Mpa$^{1/2}$, respectively, and 18.8 and 19.0 Mpa$^{1/2}$ for benzene and chloroform, respectively [17,18]. The solubility parameter of chloroform is closer to that of PLA than benzene and it is also more polar than benzene. While PI has a lower surface energy (32 mJ/m^2) than PLA (36–41 mJ/m^2) [18,19], the higher concentration of chloroform in the PLA microdomains at the air surface can balance the effective surface

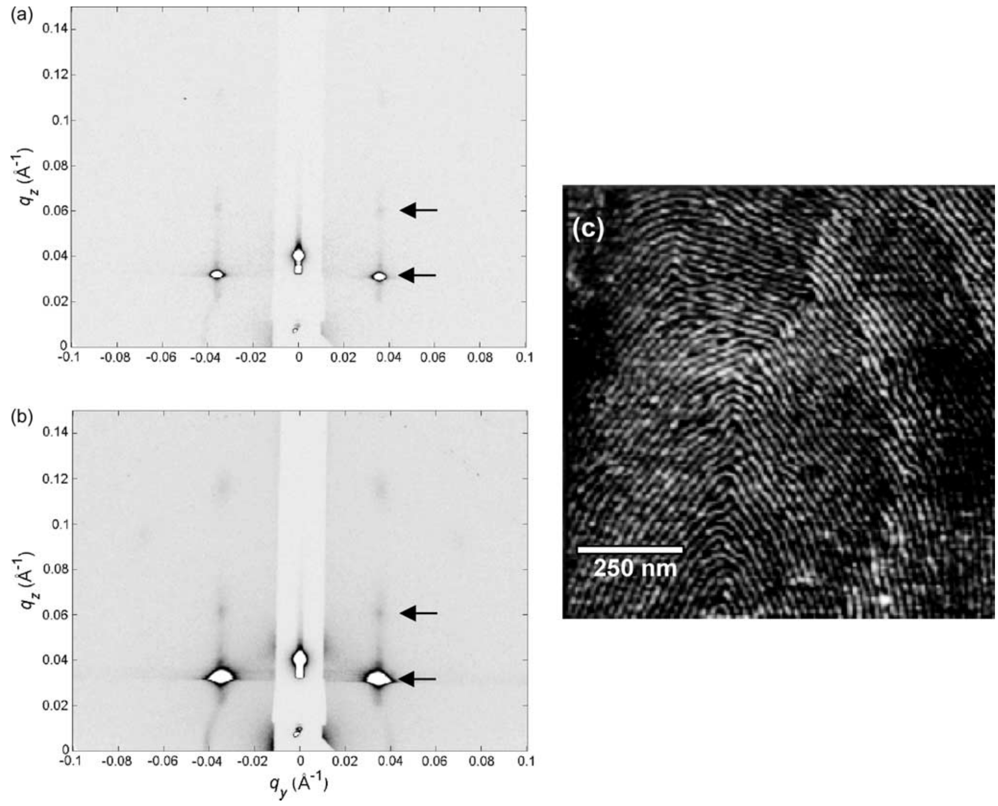

Fig. 3. GISAXS patterns at $\alpha = 0.2°$ of PI-*b*-PLA 6-3 (a) swollen with benzene and (b) after evaporation. (c) SFM phase image of the annealed unswollen film. The arrows indicate the position of the split spots from the 10 reflections.

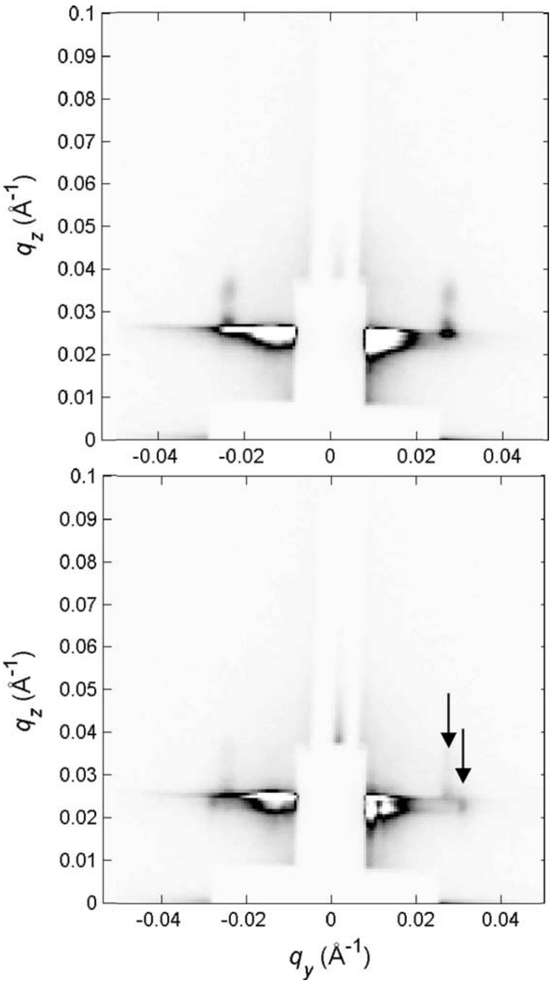

Fig. 4. GISAXS patterns at $\alpha=0.2°$ of PI-b-PLA 16-6 swollen to (a) 30 vol% and (b) 38 vol% chloroform. The arrows indicate the position of the reflections arising from parallel cylinders (smaller q_y) and perpendicular cylinders (larger q_y).

energies of the swollen blocks, allowing the perpendicular orientation to become energetically favorable.

Fig. 4 shows GISAXS patterns of a PI-*b*-PLA 16-6 film ($t_0=72$ nm) swollen to 102 nm (30 vol% chloroform, as determined from the film thickness) (Fig. 4(a)) and 116 nm (38 vol% chloroform) (Fig. 4(b)). At 30% solvent the scattering pattern indicates that the cylindrical microdomains are oriented parallel to the film surface. However, at 38% solvent two new spots appear on the equator at higher q_y, which arise from cylinders oriented normal to the film surface. Since the first order reflections of both the parallel- and perpendicular-oriented cylinders arise from the (10) planes, they should be seen at the same magnitude of q. The difference in the q_y positions of the reflections is due to the additional q_z component of the reflections from cylinders oriented parallel to the film surface. The ratio of the parallel to perpendicular peak position in q_y is $\sqrt{3}/2$, which is consistent with hexagonal packing of the cylindrical microdomains oriented parallel and perpendicular to the surface. If the films are swollen to 40 vol% chloroform, the PI-*b*-PLA will disorder but, upon solvent evaporation, cylinders oriented normal to the surface re-appear when the film thickness was 112 nm. These results are similar to those of Knoll et al., where regions in thin films of poly(styrene-*b*-butadiene-*b*-styrene) triblocks [8] showed both orientations of the cylindrical microdomains, depending upon the film thickness. In the case of PI-*b*-PLA, cylindrical microdomains oriented normal to the film surface are seen only near the disordering transition. Consequently, a high concentration of chloroform is needed to sufficiently mediate surface energies so as to orient the microdomains normal to the surface.

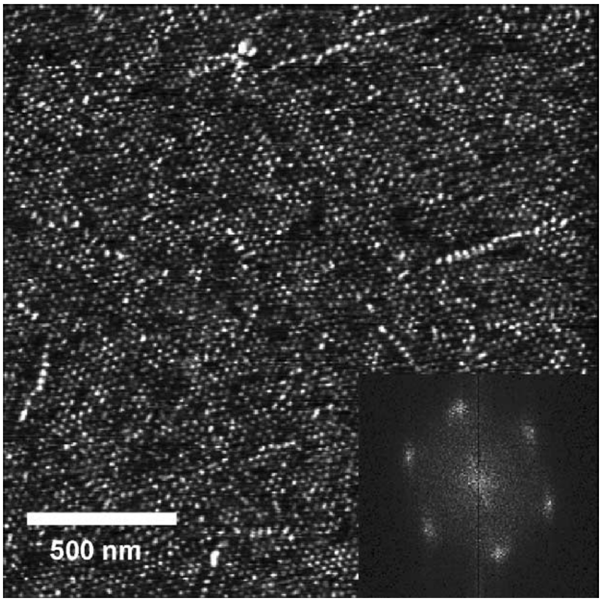

Fig. 5. SFM phase image of perpendicular cylinders in a PI-*b*-PLA thin film. The inset shows the Fourier transform of this image.

The dried film showed regions with a terraced topography which is characteristic of films where the microdomains are oriented parallel to the surface [20]. In areas of the film devoid of terracing (Fig. 5) highly ordered arrays of cylindrical microdomains oriented normal to the films surface were found. The inset shows the Fourier transform of this image and the 6-spot pattern reflects the high degree of long-range order achieved during solvent-annealing, producing grains at least 2×2 μm in size.

3. Conclusions

Using solvent annealing we have been able to control the orientation and long-range ordering of cylindrical microdomains in thin films of PI-*b*-PLA. The results show that, by judicious choice of the solvent, the orientation of the microdomains can be changed. In addition, grazing incidence small angle X-ray scattering has been shown to be a very effective tool to examine the state of orientation of the microdomains in the films during the course of solvent evaporation. This enabled the investigation of the microdomain orientation and ordering over a large range of solvent concentration and film thickness and opens an easy route to optimize the spatial organization of the microdomains in thin films.

4. Experimental

PI-*b*-PLA polymers were prepared by a previously reported method [16]. Two polymers were used in this work, PI-*b*-PLA 16-6 ($M_n = 22{,}000$, $f_{PLA} = 0.77$) and PI-*b*-PLA 6-3 ($M_n = 9000$, $f_{PLA} = 0.76$). Thin films were prepared by spin-coating polymer solutions from benzene (PI-*b*-PLA 6-3) or chloroform (PI-*b*-PLA 16-6) on silicon wafers with a native oxide surface. The initial film thickness (t_0) was measured using a Filmetrics F20 interferometer. PI-b-PLA 6-3 samples were swollen with benzene by placing them in a sealed chamber with a septum port and a connection to a dual vacuum/nitrogen line. The chamber was evacuated and refilled with nitrogen three times after which 0.1 mL of benzene was added by syringe through the septum and allowed to evaporate and swell the films for 1, 10 or 30 min. At the end of that time, nitrogen was flowed through the chamber, exiting through a needle placed in the septum, to slowly evaporate the solvent. After 20 min the films were removed from the chamber. GISAXS measurements on PI-*b*-PLA 6-3 and PI-*b*-PLA 16-6 were done using beamlines X21 and X22b, respectively, at the NSLS, Brookhaven National Labs. For swelling experiments, solvent was added to chamber by syringe (0.1–0.3 mL) and allowed to evaporate. The thickness was monitored by a Filmetrics F20 interferometer. When the solvent had completely evaporated the chamber was slowly flushed with nitrogen to evaporate the solvent. Exposures were taken for 30 s. SFM measurements were performed using a Dimension 3100 Nanoscope III SFM (Digital Instruments) in tapping mode.

Acknowledgements

We would like to thank Masc Hillmyer of the University of Minnesota for providing PI-OH homopolymer (PI-*b*-PLA 6-3) and Gregoire Cardoen and Kurt Breitenkamp for help with ethylene oxide termination. GISAXS experiments were performed at the National Synchrotron Light Source, Brookhaven National Laboratories on beamlines X21 (PI-*b*-PLA 6-3) and X22B (PI-*b*-PLA 16-6). We would like to thank Lin Yang (X21), Ben Ocko (X22B) and Oleg Gang for their assistance during GISAXS measurements. Use of the National Synchrotron Light Source, Brookhaven National Laboratory, was supported by the US Department of Energy, Office of Science, Office of Basic Energy Sciences, under Contract No. DE-AC02-98CH10886. This work was supported by the NSF sponsored Materials Research Science and Engineering Center at the University of Massachusetts, the Research Experience for Teachers program, and by Seagate Technology.

References

[1] Park C, Yoon J, Thomas EL. Polymer 2003;44:6725–60.
[2] Olayo-Valles R, Lund MS, Leighton C, Hillmyer MA. J Mater Chem 2004;14:2729–31.
[3] Liu G, Ding J, Hashimoto T, Kimishima K, Winnik FM, Nigam S. Chem Mater 1999;11:2233–40.
[4] Thurn-Albrecht T, Schotter J, Kastle GA, Emley N, Shibauchi T, Krusin-Elbaum L, et al. Science 2000;290:2126–9.
[5] Mansky P, Liu Y, Huang E, Russell TP, Hawker C. Science 1997;275: 1458–60.
[6] Horvat A, Lyakhova KS, Sevink GJA, Zvelindovsky AV, Magerle R. J Chem Phys 2004;120:1117–26.
[7] Kim SH, Misner MJ, Xu T, Kimura M, Russell TP. Adv Mater 2004;16: 226–31.
[8] Knoll A, Magerle R, Krausch G. J Chem Phys 2004;120:1105–16.
[9] Turner MS. Phys Rev Lett 1992;69:1788–91.
[10] Walton DG, Kellogg GJ, Mayes AM, Lambooy P, Russell TP. Macromolecules 1994;27:6225–8.
[11] Falsoka MJ, Banerjee P, Mayes AM, Pickett G, Balazs AC. Macromolecules 2000;33:5702–12.
[12] Huinink HP, Brokken-Zijp JCM, van Dijk MA, Sevink GJA. J Chem Phys 2000;112:2452–62.
[13] Lambooy P, Russell TP, Kellogg GJ, Mayes AM, Gallagher PD, Satija SK. Phys Rev Lett 1994;72:2899–902.
[14] Kellogg GJ, Walton DG, Mayes AM. Phys Rev Lett 1996;76:2503–6.
[15] Lee B, Park I, Yoon J, Park S, Kim J, Kim K-W, et al. Macromolecules 2005;38:4311–23.
[16] Schmidt SC, Hillmyer MA. Macromolecules 1999;32:4794–801.
[17] Van Krevelen DW. Properties of polymers. New York: Elsevier; 1997.
[18] Brandrup J, Immergut EH, Grulke EA, editors. Polymer handbook. 4th ed. New York: Wiley; 1999.
[19] Ringard-Lefebvre C, Baszkin A. Langmuir 1994;10:2376–81.
[20] Coulon G, Russell TP, Deline VR, Green PF. Macromolecules 1989;22: 2581.